TECHNICAL PAPER

Modeling Flexible Bodies with Simscape Multibody Software

An Overview of Two Methods for Capturing the Effects of Small Elastic Deformations

By S. Miller, T. Soares, Y. Van Weddingen, and J. Wendlandt

MathWorks®

Contents

1 Introduction

1.1 Why Model Flexible Bodies?

The assumption is often made in the construction of a multibody model that bodies do not deform. Each body is treated as a rigid unit, incapable of the mechanically induced distortions that real, and more compliant, materials frequently experience. The rigid-body approximation suits a wide array of multibody models. It is simple, allowing for faster simulation. It is also, in many applications, amply accurate: the material and geometry of a body are often specified so that the body does not appreciably deform.

Yet, deformation can play an important part in certain systems. Aerodynamic forces are known to induce visible flutter in aircraft wings. Impact forces often cause noticeable shudder in excavator booms. The wings and boom behave as *flexible bodies*, their deformations occasionally growing severe enough to impact the performance of their respective systems. The motions of neighboring bodies, the loads on their joints, the performance of their control algorithms, all are vulnerable to the effects of deformation.

Such effects tend to be especially pronounced in resonant systems. Resonance greatly amplifies vibrations, accelerating the rate of mechanical wear, raising power consumption, and interfering with high-precision tasks. Certain types of robotic manipulators employ active vibration control precisely for this reason—to mitigate the effect of vibrations on the positioning accuracy of the end effector. To adequately model such systems you must capture the behavior of their flexible bodies.

Figure 1: Deformation can play an important role in the dynamics of multibody systems

1.2 Two Modeling Approaches

A variety of methods exist to model flexible bodies. Among the most popular are the finite-element methods. These can be computationally expensive, however, and often require special treatment to apply to large multibody models, in particular those comprising multiple physical domains and elaborate control systems. This paper explores two practical methods that you can adopt in your Simscape Multibody™ models[1] to capture deformations that are *small*, *linear*, and *elastic*:

- **Lumped-parameter method** — Treat the flexible body as a collection of discrete flexible units. Each flexible unit comprises two or more rigid mass elements coupled by joints with internal springs and dampers. The joints provide the degrees of freedom required for deformation to occur. The mass, spring, and damper elements provide the inertial, restorative, and dissipative forces that collectively account for deformation.

- **Finite-element import method** — Treat the flexible body as the superposition of distinct rigid-body and deformation models. The rigid-body model captures the motion of the body as though it were incapable of deforming. The deformation model captures the deflections within the body as though it were fixed in place. The method derives its name from the source of much of the data behind the deformation model: a finite-element model.

1.3 The Scope of This Paper

The discussion presented here details each method, with special attention given to its workflow and parameter calculations. Some familiarity with multibody modeling is assumed. Two modeling examples are discussed—one a cantilever beam under point and distributed loads, the other a crank-slider mechanism with and without contact forces. The simulation results obtained from each method are compared to analytical predictions or, when these are unavailable, to relevant results from the scientific literature.

2 Lumped-Parameter Method

2.1 Overview

The lumped-parameter method approximates a flexible body as a collection of discrete flexible units fixed to one another. In the simple case of a long slender body, a flexible unit comprises two mass elements coupled with a joint possessing internal springs and dampers. The degrees of freedom of the joint capture the deformation modes of the flexible unit. The springs and dampers capture its stiffness and damping characteristics.

This method suits bodies with slender geometries, such as rods and beams. Figure 2 shows a simple example: a beam discretized along its length into four flexible beam units. The shaded area highlights one flexible unit. Within it are the two mass elements (m), the spring (k), and the damper (b) common to all flexible units. Rigid connections join the flexible units to their respective neighbors.

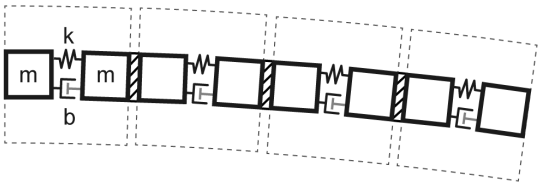

Figure 2: A flexible body according to the lumped-parameter method

2.2 Method

The lumped-parameter method comprises the four steps described below. For more information on how to perform a specific task in a Simscape Multibody model, see the Simscape Multibody documentation. Examples of multibody models based on the lumped-parameter method are available for download from the MATLAB Central™ File Exchange website.

2.2.1 Step 1: Model the Mass Elements that Comprise the Body

Each mass element accounts for a small section of the body. All are assumed rigid. The accuracy of the lumped-parameter method depends in part on the number of mass elements used. Increasing this number tends to improve the accuracy attained (albeit at a greater computational cost). In the figure, each square corresponds to a mass element.

Step 2: Connect the Mass Elements in Pairs with Joints

Each mass-joint-mass sequence represents a flexible body unit. The joints provide the degrees of freedom corresponding to the different types of deformation. Rotational degrees of freedom enable bending and torsion. Translational degrees of freedom enable axial deformation and shear. If bending is considered, the joint must lie on the neutral axis of the body.

Step 3: Add Springs and Dampers to the Various Joints

The spring and damping coefficients determine the static and dynamic deformations arising from applied forces and torques. You must calculate these coefficients from knowledge of the geometry and material properties of the beam. The calculations are outlined in sections 2.3.2 and 2.3.3.

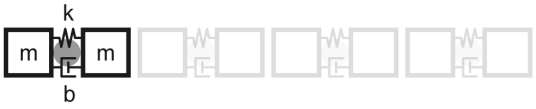

Step 4: Rigidly Connect Each Flexible Body Unit to Its Neighbors

Assemble the flexible body units into a complete flexible body by adding between them rigid connections. Each flexible beam unit that you add contributes to the body one internal degree of freedom for each type of deformation modeled. The boundary conditions of the body, imposed through joints, kinematic constraints, or explicit forces and torques, complete the model.

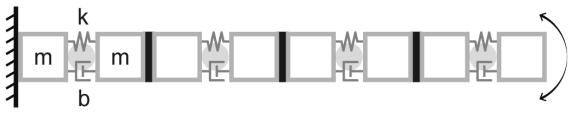

2.3 Theory

The constituents of a flexible beam unit and the relationships between them are represented in a Simscape Multibody model by means of blocks and connection lines. The challenge of the lumped-parameter method there reduces largely to the calculation of key block parameters. These include the inertial properties of the mass elements and the spring and damping coefficients of the joint. This section describes how you can obtain what are perhaps the least intuitive of these—the spring and damping coefficients.

2.3.1 Harmonic Oscillators

Consider again the beam of figure 2. Suppose for simplicity that the beam is subjected to purely longitudinal forces—that is, tension and compression in the direction of the length of the beam. A flexible beam unit then behaves as a damped harmonic oscillator with one translational degree of freedom. Holding one mass element fixed while allowing the second to translate gives, for the equation of motion,

$$m\ddot{u} + b_{\mathrm{T}}\dot{u} + k_{\mathrm{T}}u = f, \tag{1}$$

where f is the net external force acting on the translating mass element and u is the translational offset of that mass element from its equilibrium position—that corresponding to a spring in its natural length, under neither tension nor compression. Parameters m, b_{T}, and k_{T} are, respectively, the mass of a mass element, the translational damping coefficient of the joint, and the translational spring coefficient of the joint.

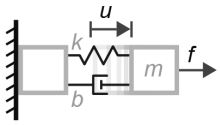

Figure 3: A flexible beam unit with one translational degree of freedom

Replacing the translational degree of freedom with a rotational degree of freedom—for example, to capture the effects of bending or twisting—gives, for the rotational form of the equation of motion,

$$I\ddot{\theta} + b_{\mathrm{R}}\dot{\theta} + k_{\mathrm{R}}\theta = \tau, \tag{2}$$

where τ is the net external torque acting on the rotating mass element and θ is the rotational offset of that mass element from its equilibrium position. Parameters I, b_{R}, and k_{R} are, respectively, the moment of inertia of a mass element about the axis of rotation, the rotational damping coefficient of the joint, and the rotational spring coefficient of the joint.

Expressing the rotational equation in terms of the often used damping ratio (ζ) and natural frequency (ω) parameters gives

$$I\left(\ddot{\theta} + 2\zeta\omega\dot{\theta} + \omega^2\theta\right) = \tau, \tag{3}$$

where

$$\zeta = \frac{b_{\mathrm{R}}}{2\sqrt{I k_{\mathrm{R}}}} \qquad \text{and} \qquad \omega = \sqrt{\frac{k_{\mathrm{R}}}{I}}. \tag{4}$$

The damping ratio is simply the fraction of the true damping coefficient, b_{R}, over the critical damping coefficient, $2\sqrt{I k_{\mathrm{R}}}$, the value at which the oscillator transitions between underdamped and overdamped conditions. The natural frequency is the rate at which an undamped oscillator tends to vibrate in the absence of an applied load. An isolated oscillator has one natural frequency. A complete flexible beam, as a composite of harmonic oscillators, has many—one for each degree of freedom provided by the joints. In the examples of section 2.4, the first four of these provide a benchmark by which to judge simulation results.

2.3.2 Spring Coefficient

In a cantilever beam subjected only to bending, the value of the spring coefficient follows from the equality between the spring torque at the joint and the bending moment on a continuous version of the flexible beam unit. Hooke's law gives the spring torque at the joint:

$$\tau_{\mathrm{k}} = k_{\mathrm{R}}\,\theta, \tag{5}$$

where τ_{k} is the spring torque, k_{R} is the rotational spring constant, and θ is the deflection angle. Classical beam theory gives the bending moment on a continuous beam unit:

$$M = \frac{E\,I_{\mathrm{A}}}{R}, \tag{6}$$

where M is the bending moment, E is Young's modulus of elasticity, I_{A} is the second moment of area, and R is the bending radius of curvature. In the limit of very small deflections, θ reduces to l/R, where l is the undeformed length of a flexible beam unit, and the spring coefficient becomes

$$k_{\mathrm{R}} = \frac{E\, I_{\mathrm{A}}}{l}. \tag{7}$$

If the flexible beam has length L and a number N of flexible beam units, then the length l of an undeformed flexible beam unit is simply

$$l = \frac{L}{N}. \tag{8}$$

Figure 4 shows the angle (θ) and radius of curvature (R) due to bending. A mass element is half the length of a flexible beam unit, $l/2$.

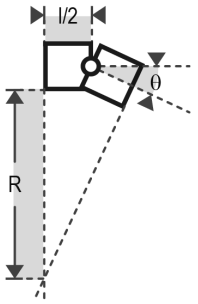

Figure 4: Geometry of a flexible beam unit with one rotational degree of freedom

The spring coefficients corresponding to other deformation types follow from a similar analysis. Table 1 summarizes the cases of axial and torsional deformation. Here, ϕ and δ are the torsional and axial deformations, k_T and k_A the torsional and axial spring constants, and G, J, and A the shear modulus, torsional constant, and cross-sectional area of the beam.

Deformation Mode	Hooke's Law	Elasticity Theory	Spring Coefficient
Torsional	$\tau_k = k_T\, \phi$	$M = GJ\phi/l$	$k_T = GJ/l$
Axial	$f_k = k_A\, \delta$	$F = EA\delta/l$	$k_A = EA/l$

Table 1: Joint spring coefficients

2.3.3 Damping Coefficient

The damping of materials is a complex phenomenon and often a challenge to characterize accurately. Sophisticated damping models exist but here a simple one is chosen. Let damping be linear and bound by

a constitutive law of the type

$$\tau_{\mathrm{b}} = b_{\mathrm{R}}\dot{\theta}, \tag{9}$$

where τ_{k} is the magnitude of the damping torque between two mass elements connected with one rotational degree of freedom. This assumption is consistent with the damping calculations of the Simscape Multibody joint blocks. As a first-order approximation, take the damping coefficient to be proportional to the spring coefficient:

$$b_{\mathrm{R}} = \alpha k_{\mathrm{R}} \tag{10}$$

The proportionality constant (α) is an empirically set damping factor. The damping coefficient then scales directly with the discretization level of the beam: increase the number of flexible beam units and the damping coefficient increases also. This scaling is provided by the spring coefficient as calculated in equations 7 and 8.

The damping factor can be set by matching the lumped-parameter deformations to reliable benchmark data. The calculated deformations should closely mirror those determined by experiment or by the simulation of a trusted model of the same body.

2.4 Examples

2.4.1 Flexible Cantilever Beam

Consider a lumped-parameter model of an aluminum cantilever beam under two loading conditions: one a distributed load provided by gravity, the other an upward point force of `20 N` applied at the free end of the beam in zero gravity (see figure 5). This model is available for download from the MATLAB® Central File Exchange. For the clear visualization of beam deformation in the distributed load case, the gravitational acceleration (g) is set there to an artificially high value of `-981 m/s`^{2}.

Beam Properties Table 2 summarizes the properties of the beam. The beam is approximately one foot in length and half an inch in width. Its construction is of aluminum. Its second moment of area is calculated from the standard analytical expression for a rectangular cross section:

$$I_{\mathrm{A}} = \frac{WT^3}{12}. \tag{11}$$

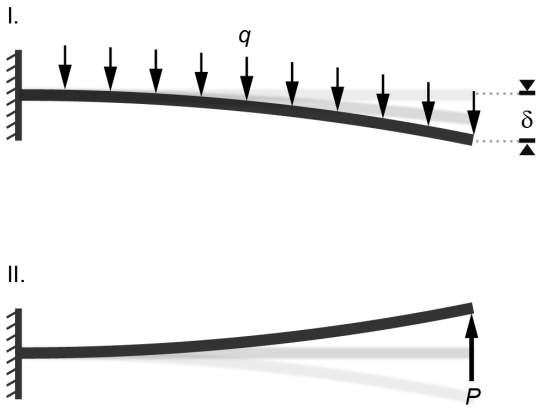

Figure 5: Cantilever beam under distributed and point loads

Length, L	Width, W	Thickness, T
`0.300 m`	`0.015 m`	`0.005 m`
Density, ρ	**Young's Modulus, E**	**Second Moment, I_{A}**
`2800 kg/m^3`	`70e9 Pa`	`1.563e-10 m^4`

Table 2: Cantilever beam properties

Model Parameters The beam model considered here comprises ten flexible beam units arranged in sequence with one end fixed to the world. Table 3 summarizes the properties of a flexible beam unit. See section 2.3.2 for more on the spring coefficient calculation and section 2.3.3 for more on the damping coefficient calculation. The elastic damping factor (from which the damping coefficient derives) is tuned using the finite-element model behind the example of section 3.5.1. Its value is `2.58e-5 s`.

Length, L/N	Stiffness, k_{R}	Damping, b_{R}
`0.03 m`	`3.65e2 N·m/rad`	`9.41e-3 N·m/(rad/s)`

Table 3: Flexible beam unit properties

Analytical Deflections Consider as a first benchmark the equilibrium tip deflection predicted from theory for each loading configuration. For a cantilever beam subjected to a uniform gravitational load,

$$\delta = \frac{mg}{L}\frac{L^4}{8EI_{\mathrm{A}}} = -0.0191 \text{ m}, \tag{12}$$

where the term $\frac{mg}{L}$ is the gravitational force acting on a unit length of the beam under the assumption that $g = -981$ m/s^2. For a cantilever beam subjected to a point force applied at the tip in a zero-gravity environment,

$$\delta = \frac{PL^3}{3EI_{\mathrm{A}}} = 0.0165 \text{ m}, \tag{13}$$

where P is the point force, chosen here to have a magnitude of 20 N.

Analytical Frequencies Consider as a second benchmark the set of natural frequencies ω_i predicted from theory for the cantilever beam in the undamped, unloaded case:

$$\omega_i = \left(\frac{\alpha_i}{L}\right)^2 \sqrt{\frac{EI_A}{\rho A}}, \tag{14}$$

where i are the indices of the free vibration modes and α_i the multipliers specific to those modes, defined as the ith roots of the transcendental equation

$$1 + cos\,(\alpha)\,cosh\,(\alpha) = 0. \tag{15}$$

For a cantilever beam, the first four values of α_i are `1.875`, `4.694`, `7.855`, and `10.996`, yielding, for the first four modes, the natural frequencies

$$\omega_{\mathrm{I}} = 281.91 \text{ rad/s}, \qquad \omega_{\mathrm{II}} = 1766.82 \text{ rad/s}, \qquad \omega_{\mathrm{III}} = 4947.65 \text{ rad/s}, \qquad \omega_{\mathrm{IV}} = 9695.64 \text{ rad/s}.$$

In units of Hertz (using the equality $f_i = \omega_i/2\pi$),

$$f_{\mathrm{I}} = 44.87 \text{ Hz}, \qquad f_{\mathrm{II}} = 281.20 \text{ Hz}, \qquad f_{\mathrm{III}} = 787.44 \text{ Hz}, \qquad f_{\mathrm{IV}} = 1543.11 \text{ Hz}.$$

Simulated Deflections Figure 6 shows the time-varying deflections of the free end of the beam under a distributed gravitational load (case **I**) and an upward point force applied at the tip (case **II**). The beam is lightly damped and reaches equilibrium in each case after approximately five seconds. The point force is removed after five seconds of simulation, allowing the beam to return to its natural state of zero deflection. The return to equilibrium is governed by the internal spring and damping torques of the beam alone—gravity is ignored.

The simulation results show that the free end of the beam settles at an equilibrium deflection of `-0.0183 m` under a uniform gravitational load and `0.0164 m` under an upward-facing point load. Compare these values

to the analytical predictions of `-0.0191 m` for a uniform gravitational load and `0.0165 m` for an upward-facing point load, respectively.

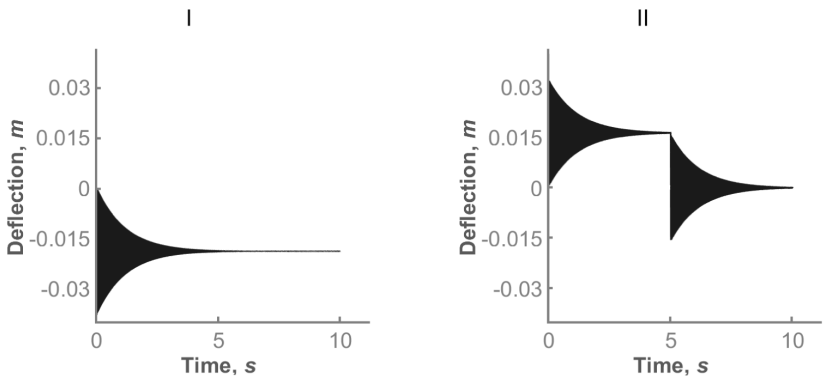

Figure 6: Tip deflection due to a distributed gravitational load (left) and to an upward point load (right)

Simulated Frequencies Figure 7 shows the first four vibration mode shapes of the cantilever beam (labeled **I** through **IV**). The mode shapes result from the modal analysis of a linearized lumped-parameter model with zero damping. Their frequencies closely match those predicted from theory:

$$f_{\mathrm{I}} = 44.87 \text{ Hz}, \qquad f_{\mathrm{II}} = 281.60 \text{ Hz}, \qquad f_{\mathrm{III}} = 789.17 \text{ Hz}, \qquad f_{\mathrm{IV}} = 1547.27 \text{ Hz}.$$

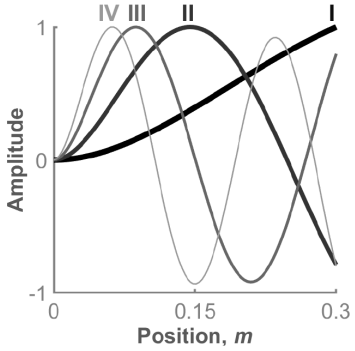

Figure 7: Schematic of the (normalized) beam mode shapes

2.4.2 Crank-Slider with Flexible Links

Consider a crank-slider mechanism with flexible crank and coupler (or *connecting*) links with and without contact. This example illustrates the application of the lumped-parameter method to a more complicated, closed-chain, system. It, too, is available for download from the MATLAB® Central File Exchange.

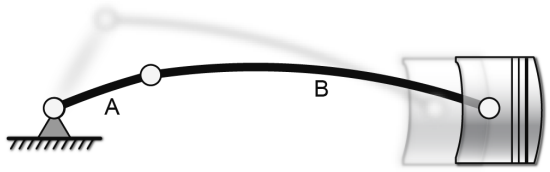

Figure 8: Crank-slider mechanism with flexible crank (**A**) and coupler (**B**) links

For comparison purposes, the model is configured with the material and geometry properties described in a case study published by A. Shabana[2]. The crank shaft is driven by an applied torque of the form

$$M(t) = \begin{cases} 0.01\left(1 - e^{\frac{-t}{0.167}}\right) & t < 0.70s \\ 0 & t \geq 0.70s \end{cases}, \tag{16}$$

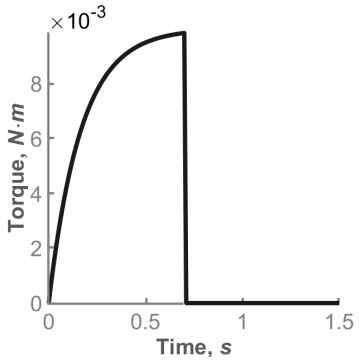

Figure 9: Driving torque applied at the crank joint

Link Properties Table 4 summarizes the properties of the crank and coupler links. The coupler is approximately one foot in length and the crank half a foot. The links have the same cross-sectional geometry and density but different moduli of elasticity, with the crank being just over one order of magnitude stiffer than the coupler.

Link	Length, L	Width, W	Thickness, T
Crank	`0.152 m`	`0.0091 m`	`0.0087 m`
Coupler	`0.304 m`	`0.0091 m`	`0.0087 m`
Link	**Density, ρ**	**Young's Modulus, E**	**Second Moment, I_A**
Crank	`2770 kg/m^3`	`1e9 Pa`	`4.909e-10 m^4`
Coupler	`2770 kg/m^3`	`5e7 Pa`	`4.909e-10 m^4`

Table 4: Crank and coupler link properties

Model Parameters The crank and coupler are modeled as flexible beams each rectangular in cross section. The crank comprises ten flexible beam units and the coupler twenty. The flexible beam units have one rotational degree of freedom each, about an axis that is simultaneously perpendicular to the (vertical) gravity vector and to the (horizontal) path of the slider.

Table 5 summarizes the properties of an individual flexible beam unit. See section 2.3.2 for more on the spring coefficient calculation and section 2.3.3 for more on the damping coefficient calculation. The elastic damping *factors* (from which the damping coefficients derive) are tuned using the finite-element model behind the examples of section 3.5.2. Their values are `3.38e-5 s` for the crank and `6.03e-4 s` for the coupler.

Link	Length, L/N	Stiffness, k_R	Damping, b_R
Crank	`0.0152 m`	`32.30 N·m/rad`	`1.09e-3 N·m/(rad/s)`
Coupler	`0.0152 m`	`1.61 N·m/rad`	`9.74e-4 N·m/(rad/s)`

Table 5: Flexible beam unit properties

Simscape Multibody Model Figure 10 shows a Simscape Multibody model of the crank-slider mechanism. The crank and coupler are both modeled using the lumped-parameter method. The various bodies connect to each other and to the world by means of joints. The driving torque is applied directly to the world-crank revolute joint and the hard-stop force is applied directly to the slider-world prismatic joint.

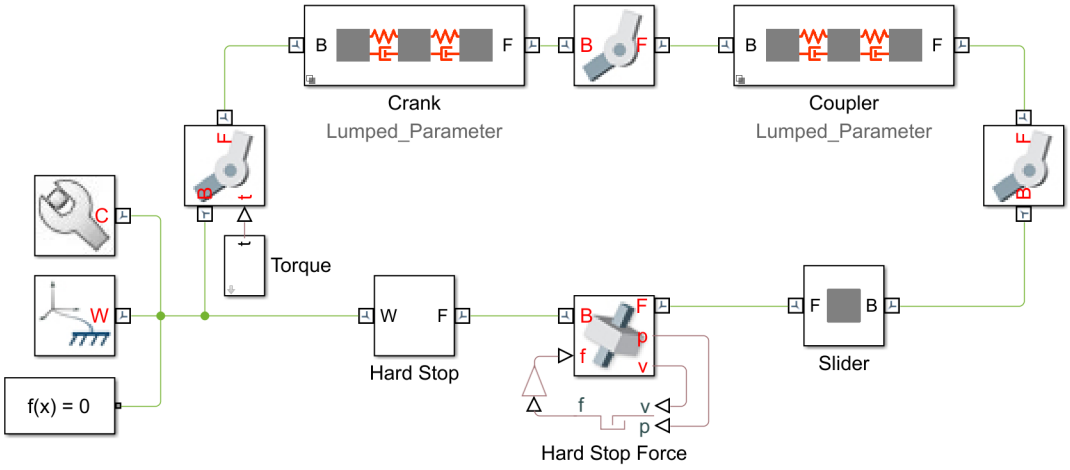

Figure 10: Simscape Multibody model of a crank-slider mechanism

Figure 11 shows a Simscape Multibody model of one flexible body—the coupler. For simplicity, the model is shown with only four flexible beam units. These are each enclosed in a Simulink Subsystem block (named **Flexible Unit 1–4**). Two Rigid Transform blocks (**Rigid Transform A–B**) define the placement of the connection frames (**B** and **F**) of the body—those through which it connects to the remainder of the model.

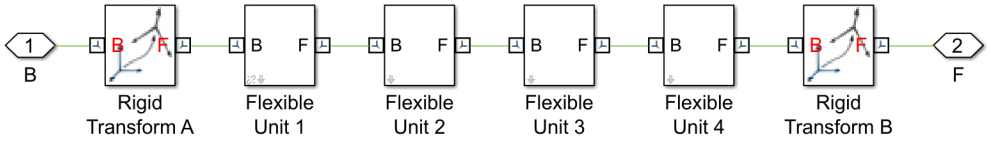

Figure 11: Simscape Multibody model of a flexible coupler

Within each flexible beam unit are additional blocks representing its constituent components. Two Solid blocks (named **Mass 1–2**) represent the mass elements of the flexible beam unit. They are connected by a Revolute Joint block (**Joint**) within which are the spring and the damper needed to capture compliant behavior. The properties of the flexible beam unit are specified as parameters of these blocks.

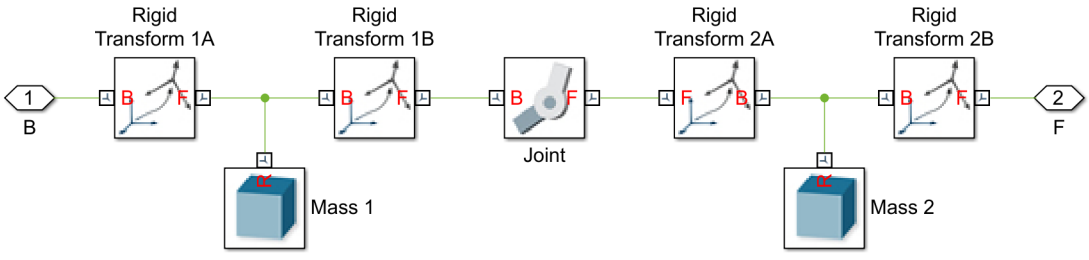

Figure 12: Simscape Multibody model of a flexible beam unit

The four Rigid Transform blocks (Rigid Transform 1A–2B) merely define the placement of the various

connection frames—those through which the mass elements connect to each other and those through which the flexible beam unit connects to its neighbors.

Simulated Deflections Figure 13 overlays the simulation results obtained using the lumped-parameter method (curve **B**) on those published by A. Shabana (curve **A**). The curves each correspond to the transverse deflection measured at the midpoint of the coupler link with respect to an imaginary line drawn between the longitudinal ends of the same link.

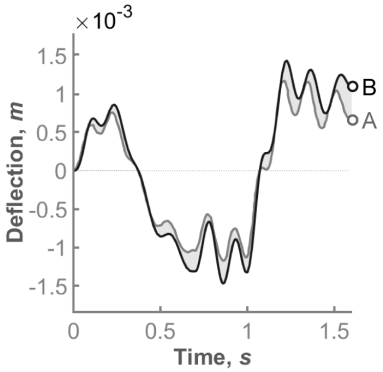

Figure 13: Comparison to Shabana[2] simulation results (**A**: Shabana, **B**: Simscape Multibody)

Figure 14 shows the simulation results obtained from a model with an obstacle—a translational hard stop—placed in the path of the slider. Contact occurs shortly after the 0.5-second mark, inducing in the coupler link the vibrations shown. As before, the results correspond to the transverse deflection measured at the midpoint of the coupler link. The oscillations decay at a rate determined by the damping coefficient used in the model.

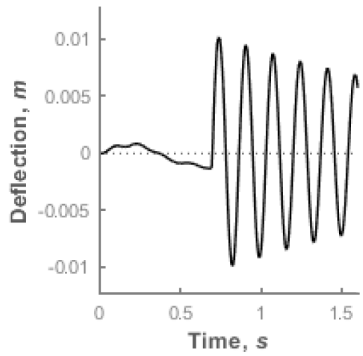

Figure 14: Coupler deflection due to contact

Simulation Accuracy The simulation results depend closely on the number of flexible beam units used in the model. Figure 15 compares the simulation results, in a model without an obstacle, for different crank and coupler discretizations. Curves **A**, **B**, **C**, and **D** correspond, respectively, to a crank with two, five, ten, and twenty flexible beam units and to a coupler with four, ten, twenty, and forty.

The simulated deflections approach those obtained by A. Shabana as the crank and coupler become more finely discretized. At twenty flexible beam units in the crank and forty in the coupler only a small discrepancy remains. This discrepancy may reflect a failure by the lumped-parameter method to precisely capture the instantaneous curvature of the beam (upon which the bending moment depends). The results published by A. Shabana are overlaid in bold (beneath curve **D**).

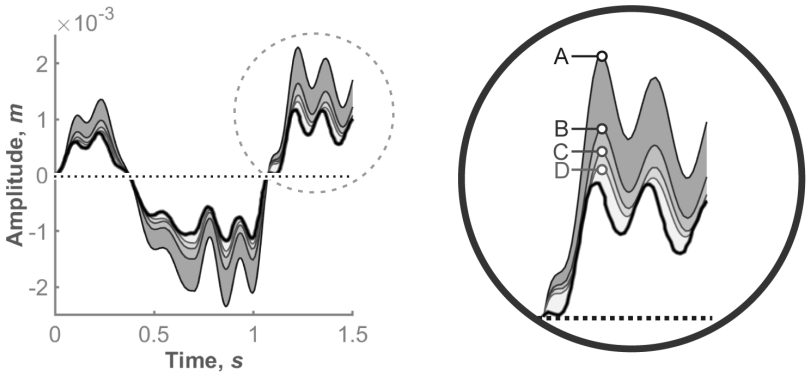

Figure 15: Effect of changing the level of discretization of the flexible bodies (**A**: 4-element coupler, **B**: 10-element coupler, **C**: 20-element coupler, **D**: 40-element coupler)

Visualization Results Figure 16 shows the visualization results obtained from a Simscape Multibody model of the crank-slider mechanism. The coupler is modeled as a rigid body in case I, as a flexible body with two flexible beam units in case II, and as a flexible body with ten flexible beam units in case III. In each case, the model is shown as it appears an instant (`0.05 s`) after collision with the hard stop.

Figure 16: Simscape Multibody visualization results for the lumped-parameter method (**I**: rigid coupler, **II**: 2-element flexible coupler, **III**: 10-element flexible coupler)

The coupler is naturally undeformed in case I. It is slightly deformed in case II but, due to the small number of flexible beam units, its visualization is rough in appearance. The same deformation is evident in case III, now with smoother visualization results produced by the greater number of flexible beam units.

3 Finite-Element Import Method

3.1 Overview

The finite-element import method approximates a flexible body as the superposition of a *rigid-body* model and a *deformation* model (their motions shown in figure 17). The rigid-body model captures the rotation and translation of the body as if it did not deform at all. It is, by itself, a complete representation of a body. In a Simscape Multibody model, it bears little difference from any other body, with frames, geometry, and inertia included among its attributes.

The deformation model calculates the elastic deflections at selected points throughout the body as though the body had been pinned in place. The deformation model is merely an addition to the rigid-body model—a state-space system, not unlike those used in control applications, and whose parameters are derived in part from a finite-element model. The two models connect through separate components known as *deflection joints* (figure 18).

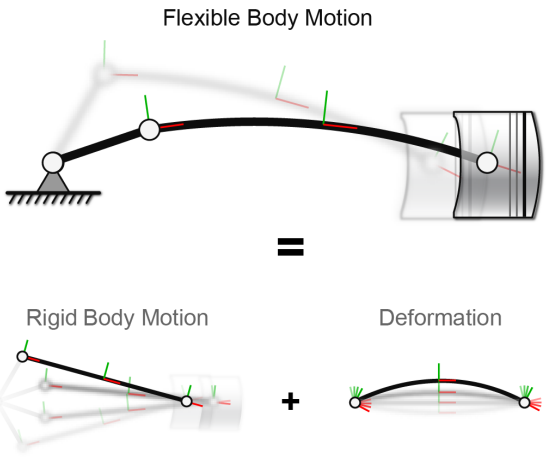

Figure 17: Flexible body motion as a superposition of rigid body motion and deformation

Note The accuracy of this method depends on the spatial distribution of the mass properties of the body. These include not only mass but also the center of mass, moments of inertia, and products of inertia. While constant in a rigid body, they can change in a flexible body and therefore impact your simulation results. You can improve these results by splitting the mass properties into portions spread throughout the span of the body. Ways in which you can do this, and the rationale for each, are discussed in section 3.3.2.

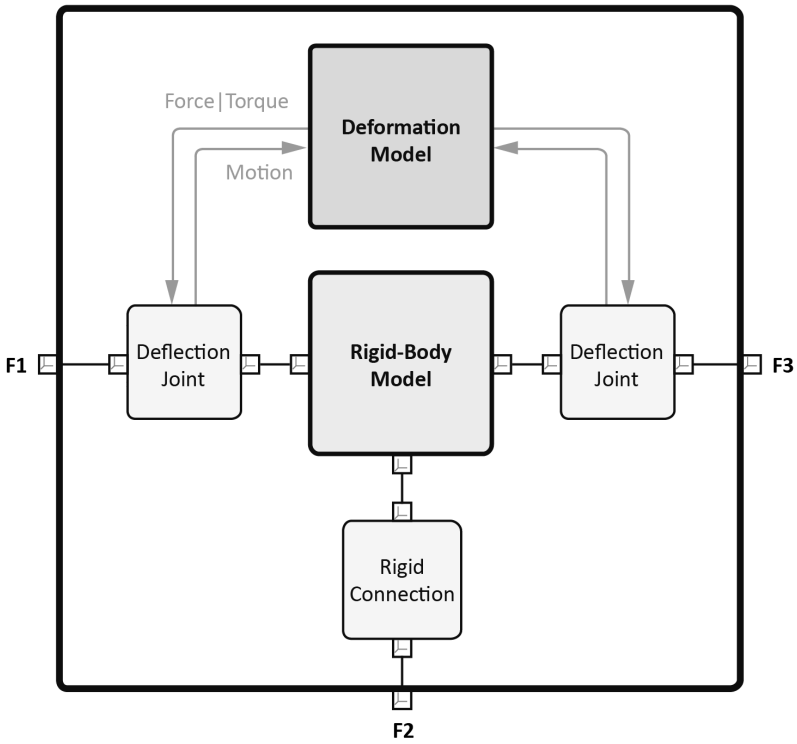

Figure 18: A flexible body according to the finite-element import method

3.1.1 Deformation Model

Consider briefly how the deformation model recasts a finite-element model in state-space form. A finite-element model discretizes the body into a polygonal mesh with numerous vertices, or *nodes*, each with as many as six degrees of freedom. The mesh is governed, in the undamped case, by the equation of motion

$$\boldsymbol{M}\ddot{\mathbf{u}}_{\mathrm{d}} + \boldsymbol{K}\mathbf{u}_{\mathrm{d}} = \mathbf{f}, \tag{17}$$

where $\boldsymbol{M}$ is the mass matrix of the discretized body, $\boldsymbol{K}$ is its stiffness matrix, $\mathbf{u}_{\mathrm{d}}$ is the array of its nodal degrees of freedom, and $\mathbf{f}$ is the array of all external loads acting at its nodes. The state-space representation replaces this second-order differential equation with a system of first-order equations—the state equation,

$$\dot{\mathbf{x}} = \boldsymbol{A}\mathbf{x} + \boldsymbol{B}\mathbf{u}, \tag{18}$$

and the output equation,

$$\mathbf{y} = \boldsymbol{C}\mathbf{x} + \boldsymbol{D}\mathbf{u}, \tag{19}$$

where **x**, **u**, and **y** are the state, input, and output vectors, and $\boldsymbol{A}$, $\boldsymbol{B}$, $\boldsymbol{C}$, and $\boldsymbol{D}$ are the state, input, output, and direct feedthrough matrices. These matrices are calculated here from the mass, damping, and stiffness matrices obtained from a *reduced* finite-element model. The calculations are described in detail in section 3.4.4.

Reduced Models The process of reducing a model eliminates from it a large number of degrees of freedom. In the treatment presented here, these are equal in number to the degrees of freedom of the eliminated nodes. In the model reduction method considered here, they correspond to fixed-boundary vibration modes, namely those in the high end of the frequency range, whose amplitudes are negligible—and whose impact on nodal deflections therefore is too.

Reduced models are advantageous for two reasons. First, they are computationally simpler and therefore conducive to faster simulation. Second, because the degrees of freedom of which they have been stripped correspond only to the highest-frequency, lowest-amplitude vibration modes, they are also amply accurate for a variety of use cases.

The few nodes that remain in the model suffice to connect the body to joints and other kinematic constraints. These nodes are referred to as *boundary* nodes and they collectively map to the *interface frames* (described in the following section) of the final model.

For a discussion of a model reduction method known as the Craig-Bampton method, see section 3.4.1.

3.1.2 Interface Frames

Frames are axis triads, each with an origin, used in multibody models to resolve the positions of bodies and of points within them. They are often referred to as coordinate systems. Their origins each encode a position and their axes an orientation. Frames play a critical role in Simscape Multibody software, where they are especially prominent in the representations of bodies.

Interface frames are the special subset that you select in a flexible body for the calculation of deformation. They encompass all points of utility—those intended for connection to other bodies, for the application of forces and torques, or for the sensing of motion. They each correspond to a boundary node in the reduced finite-element model.

There are few constraints on the number of interface frames (or, equivalently, of boundary nodes). To adequately capture deformation, a minimum of three is recommended. This minimum may vary with the body and its intended use. A body with many joint connections naturally requires more interface frames than one with few. The schematic of figure 18 corresponds to a model with three (**F1**, **F2**, and **F3**).

3.1.3 Deflection Joints

As the natural points of connection to other bodies, interface frames often attach to joints that are external to the flexible body. These are the joints that, in a typical multibody model, link bodies into articulated

systems. In a crank-slider mechanism, for example, they include the revolute joints between the crank and the coupler and between the coupler and the slider.

Interface frames connect to a second set of joints, however. These are internal to the flexible body and do not correspond to physical joints between bodies. Their sole purpose is to capture deflection against a reference frame affixed to the rigid-body model. These are the deflection joints introduced in section 3.1. The schematic of figure 18 corresponds to a model with two. These joints work by:

a) *Providing the degrees of freedom required for deflection.* In the most general case, each deflection joint provides six degrees of freedom between an interface frame and the corresponding connection frame on the rigid-body model.

b) *Sensing the deflections of the interface frames relative to the frames of the rigid-body model.* The sensing signals (position, velocity, acceleration) are important as inputs to the deformation model.

c) *Applying to the interface frames the forces and torques associated with their deflections.* The forces and torques arise from joint actuation inputs provided by the deformation model and serve to resist continued deflection.

Note that the deformation model is a state-space representation and that it has no frames by which to connect to deflection joints. Instead, the deformation model connects to the deflection joints by means of signals arranged in a feedback loop. This loop comprises the last two items of the previous list.

3.1.4 Reference Frame

Recall that the rigid-body model is designed to capture only rigid-body motion, and the deformation model only deformation. The deformation model isolates deformation from rigid-body motion by performing its calculations against a reference frame fixed to the rigid-body model. It is convenient to select as the reference frame one of the interface frames, in which case the associated deflection is always zero.

Fixing an interface frame in a state of zero deflection is equivalent to removing the degrees of freedom from its deflection joint—and therefore to replacing that joint with a rigid connection. Such a connection is denoted in figure 18 as “Rigid Connection” (frame **F2**). You must define exactly one reference frame.

Your choice of reference frame can impact the simulation results. Reference frames placed near the center of the body often lead to more accurate simulation results. If necessary, consider adding an additional boundary node to your reduced finite-element model in order to accommodate the definition of such a reference frame.

You must also fix—or remove the degrees of freedom of—the corresponding boundary node in your reduced finite-element model. You can do this as described in section 3.4.2. The basic principle is simple: to remove from the governing equation of motion all matrix and vector elements associated with the fixed boundary node. The effect is to eliminate from the model the degrees of freedom originally associated with the node.

3.2 Method

The finite-element import method comprises the five steps described below. For more information on how to perform a specific task in a Simscape Multibody model, see the Simscape Multibody documentation.

Examples of multibody models based on the finite-element import method are available for download from the MATLAB® Central File Exchange website.

Step 1: Plan the Placement of the Reference Frame and Boundary Nodes of the Body

Decide where to place the reference frame of the flexible body. The finite-element import method involves as many as three modeling environments: CAD, finite-element, and multibody. To obtain meaningful results, it is essential that the reference frame be the same in all those that you use.

Consider also the points on the body that you will later need for connection in a model, for the application of force or torque, or for the sensing of motion. Each must correspond to a boundary node in the reduced finite-element model and to an interface frame in the flexible body representation that you add to your multibody model.

The figure shows a body with geometry derived from a CAD model—the most common source of geometry data. Three finite-element boundary nodes are shown: **N1**, **N2**, and **N3**. Two (**N1** and **N3**) identify multibody connection points. Another (**N2**) identifies a central location suited for defining the reference frame.

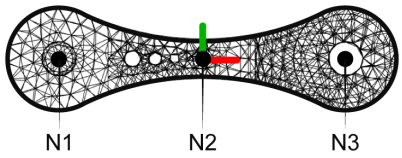

Step 2: Create the Rigid-Body Model and Add Frames Representing the Boundary Nodes

Model the body as a rigid component in your multibody modeling environment. In Simscape Multibody, you create such a model by connecting solids through frames, rotating and translating these as needed to obtain the desired placement. The solids collectively provide the mass properties of the body.

Add one frame for each boundary node in your reduced finite-element model. These are the interface frames of the flexible body in its undeformed state. Ensure that the origin of each frame has the same location as the boundary node on which it is based and the same orientation as the reference frame.

The figure shows an example with three interface frames (**F1**, **F2**, **F3**) based on the boundary nodes decided upon (**N1**, **N2**, **N3**).

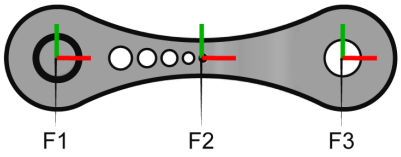

Step 3: Place Deflection Joints Between the Rigid-Body Model and the Interface Frames

Attach a joint to each interface frame with the exception of one. The joints are those described in section 3.1.3—the deflection joints. They capture the displacements of the interface frames of the flexible body relative to those defined in step 2, their counterparts in the undeformed state. Configure each deflection joint for connection to the state-space representation that you later create. Select:

- Position, velocity, and acceleration as the joint sensing outputs
- Force and torque as the joint actuation inputs

The degrees of freedom of the deflection joints determine the types of deformation that the body is capable of. Use joints with six degrees of freedom to capture all possible types of deformation. The interface frame left without a deflection joint serves as the zero-deflection reference in your model. The deflections of all other interface frames are defined against this reference. For more information, see sections 3.1.4 and 3.4.2.

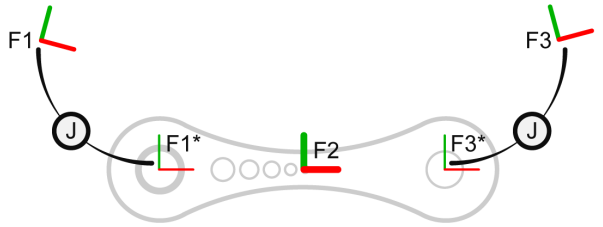

Step 4: Create the Deformation Model and Connect It to the Deflection Joints

Formulate the state-space system introduced in section 3.1.1:

$$\dot{\mathbf{x}} = \boldsymbol{A}\mathbf{x} + \boldsymbol{B}\mathbf{u} \qquad \text{and} \qquad \mathbf{y} = \boldsymbol{C}\mathbf{x} + \boldsymbol{D}\mathbf{u}. \tag{20}$$

Determine the state-space matrices ($\boldsymbol{A}$, $\boldsymbol{B}$, $\boldsymbol{C}$, and $\boldsymbol{D}$) in terms of the mass, stiffness, and damping matrices of your reduced finite-element model. The matrix calculations are detailed in section 3.4.4.

The state-space system is your deformation model. In Simulink®, you can represent a state-space system using the State-Space block. Use the motion sensing outputs from the deflection joints as the inputs to your state-space system. Use the force and torque outputs from the state-space system as the inputs to your deflection joints.

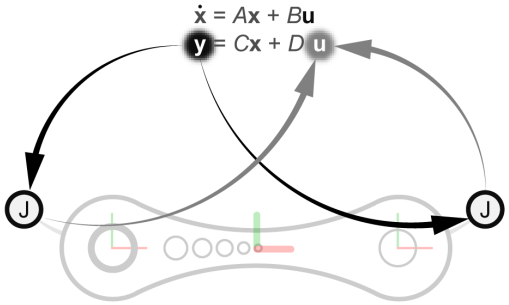

Step 5: Extract the Reduced Mass and Stiffness Matrices from the Finite-Element Model

Configure the finite-element model of the flexible body using your preferred finite-element application. Ensure that the reference frame matches the frame previously established for the rigid body and deformation models. Ensure also that the boundary nodes in your finite-element model correspond to the interface frames in the rigid-body model.

Finally, configure the number of vibration modes to retain and generate the reduced finite-element model. Extract the mass, stiffness, and, if provided, damping matrices and add them as parameters to the state-space representation of the deformation model. These matrices are used in the calculation of the various state-space matrices.

3.3 Guidelines

3.3.1 Algebraic Loops

As noted in section 3.1.3, deflection joints each connect to the deformation model via a feedback loop. If a feedback loop is such that the output of a calculation at a time step depends on its own value at that time step, that feedback loop is also an *algebraic loop*. Algebraic loops can be difficult to solve and often slow down simulation.

In Simulink terms, an algebraic loop is one that consists entirely of direct-feedthrough blocks—those whose outputs at a time step depend directly on their inputs at that time step. You can break a Simulink algebraic loop by adding to it a block that does not behave as direct-feedthrough.

A suitable option in a Simscape Multibody model is the Simulink Transfer Fcn block. Simply insert the block in the algebraic loop and use its parameters to specify the first-order transfer function

$$\frac{1}{\tau s + 1}, \tag{21}$$

where τ is a characteristic time constant—a measure of the time taken by the output signal to reach 63% of its steady-state value when given a step input signal.

The addition of a transfer function to an algebraic loop introduces in that loop a slight time delay. The delay is proportional to the characteristic time constant and it can, in certain cases, significantly impact the transient response of the model. You can mitigate such an impact by specifying a sufficiently small time constant.

For the most accurate results, the time constant should be no greater than half the period of the fastest oscillation mode in your model. Start with a value an order of magnitude smaller and fine-tune it if necessary. Avoid values that are much smaller as these can negatively impact the speed of simulation.

3.3.2 Interface Inertias

The interface frames of a flexible body connect internally to deflection joints and externally to multibody joints, those placed not within but between bodies. Because the interface frames have no inertia of their own, you must rigidly connect to each a component that does. Every joint should connect on each side to an inertia and this step helps to fulfill this requirement. You can conceive of the interface inertias in different ways:

a) As modeling artifacts introduced to prevent simulation errors and to ensure a reasonable simulation speed. The interface inertias are negligible and do not correspond to a physical part of the flexible body. The inertial properties should be neither so large as to impact model dynamics nor so small as to allow simulation errors to occur.

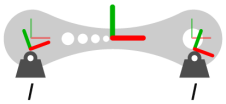

b) As small sections of the flexible body, such as the tips, or ends, at which a mechanical link connects to other bodies. The interface inertias are small and correspond to a physical portion of the body.

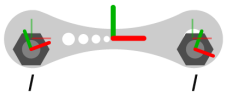

c) As sizeable sections of the flexible body, split from the rigid-body model to more precisely reflect the distribution of inertia during deformation. The interface inertias are substantial and correspond to a physical part of the body.

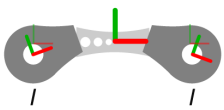

Option c produces the most accurate simulation results. The reason is two-fold. Partly, the mass properties of a flexible body change as it deforms. These are, however, specified as constants in the rigid-body model

and a discrepancy therefore arises between simulation and the physical world. Splitting the mass properties over the interface frames allows you to more closely capture their distribution during deformation.

Note also that the rigid-body model is fixed only to the reference frame. An external force applied there has to overcome the full inertia of the body. The same is not true of an external force applied at a different interface frame. Splitting the mass properties over the interface frames allows you to more evenly distribute their effects and correct for this issue.

3.3.3 Body Visualization

One interface frame must serve as reference for the measurement of deflection. The reference frame is chosen to be coincident with an interface frame and its deflection is therefore always zero. This convention is enforced by removing from the frame all of its deflection degrees of freedom—that is, by ensuring that the interface frame connects to the rigid-body model not through a deflection joint but through a rigid connection.

Your selection of reference frame impacts your visualization results. Figure 19 shows an example: a binary link with three interface frames, two at its ends and one at its center. The reference frame is at the leftmost end in case I, at the center in case II, and at the rightmost end in case III. The shaded areas depict the geometry of the body in the undeformed configuration. They correspond to the rigid-body model. The curved lines depict the interface frames in a deformed configuration. They correspond to the deformation model.

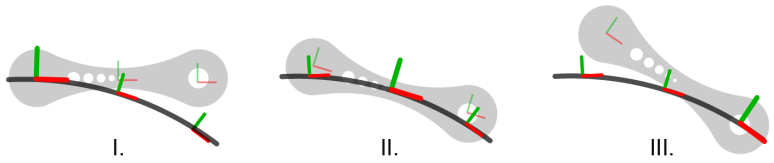

Figure 19: Flexible body visualization with reference frame at different locations

Note that the interface frames (through which the body connects to its neighbors) lie on the curved lines corresponding to the deformation model. Deformation is shown as identical in all three cases. The placement of the rigid-body model varies significantly from case to case and causes deformation to appear to differ. In addition, because the displacements of the deflection joints are measured against different reference frames, these too may differ. Splitting the inertia of the body into sizeable portions and assigning a geometry to each generally improves the visualization results.

3.4 Theory

The constituents of a flexible-body model and the relationships between them are represented in a Simscape Multibody model by means of blocks and connection lines. The most noteworthy of these is perhaps the Simulink State-Space block that in the examples of section 3.5 comprises the deformation model. The challenge of the finite-element import method reduces largely, in this case, to the calculation of the State-Space block parameters. These include the $\boldsymbol{A}$, $\boldsymbol{B}$, $\boldsymbol{C}$, and $\boldsymbol{D}$ matrices of the state-space system

given by equations (18) and (19). This section describes how you can reduce a finite-element model and, from its mass, stiffness, and damping matrices, obtain the required state-space matrices.

3.4.1 Model Reduction

Recall from the discussion of section 3.1.1 that the state-space matrices derive from a reduced form of a finite-element model. This paper focuses on a model reduction method first presented in 1968 by R. Craig and M. Bampton[3]. This method has since found widespread application in the analysis of multibody problems. Its use of boundary nodes, and the direct mapping of these to interface frames, makes it especially convenient for the finite-element import method.

A model reduction method serves to reduce the complexity (and therefore size) of a model. The Craig-Bampton method achieves this reduction by eliminating all fixed-boundary vibration modes whose frequencies are above a certain cutoff. The result is a simplified model, with fewer variables, and with smaller mass and stiffness matrices. You can, by carefully selecting the cutoff frequency, preserve the essential dynamic characteristics of the model.

The Craig-Bampton method generally proceeds as follows:

1. **Split** the nodes of a finite-element mesh into internal and boundary sets.
2. **Express** the degrees of freedom of the partitioned nodes in terms of boundary and modal coordinates.
3. **Truncate** the set of modal coordinates at a designated cutoff frequency.
4. **Reformulate** the model in terms of the reduced degrees of freedom—the physical coordinates of the boundary nodes and the truncated modal coordinates.

From the discussion of section 3.1.1, the undamped nodal motions in a finite-element mesh can be expressed as

$$\boldsymbol{M}\ddot{\mathbf{u}}_{\mathrm{d}} + \boldsymbol{K}\mathbf{u}_{\mathrm{d}} = \mathbf{f}. \tag{22}$$

Partitioning the nodes into internal and boundary sets yields

$$\begin{bmatrix} \boldsymbol{M}_{bb} & \boldsymbol{M}_{bi} \\ \boldsymbol{M}_{ib} & \boldsymbol{M}_{ii} \end{bmatrix} \begin{bmatrix} \ddot{\mathbf{u}}_b \\ \ddot{\mathbf{u}}_i \end{bmatrix} + \begin{bmatrix} \boldsymbol{K}_{bb} & \boldsymbol{K}_{bi} \\ \boldsymbol{K}_{ib} & \boldsymbol{K}_{ii} \end{bmatrix} \begin{bmatrix} \mathbf{u}_b \\ \mathbf{u}_i \end{bmatrix} = \begin{bmatrix} \mathbf{f}_b \\ \mathbf{f}_i \end{bmatrix}, \tag{23}$$

where the subscript b refers to the boundary nodes and the subscript i refers to the internal nodes. Expressing the degrees of freedom of the partitioned nodes in terms of boundary and modal coordinates (by the so-called Craig-Bampton transformation) gives

$$\begin{bmatrix} \mathbf{u}_b \\ \mathbf{u}_i \end{bmatrix} = \boldsymbol{H} \begin{bmatrix} \mathbf{u}_b \\ \boldsymbol{\eta} \end{bmatrix}, \tag{24}$$

where $\boldsymbol{\eta}$ is the set of modal degrees of freedom—the modal amplitudes resulting from the assumption that the boundary nodes are fixed. The degrees of freedom in $[\mathbf{u}_b \ \boldsymbol{\eta}]$ form a hybrid set, with some ($\mathbf{u}_b$) defined in physical space and some ($\boldsymbol{\eta}$) defined in modal space. $\boldsymbol{H}$ is the Craig-Bampton transformation matrix,

$$\boldsymbol{H} = \begin{bmatrix} \Xi & \boldsymbol{\Phi} \end{bmatrix}, \tag{25}$$

where Ξ is a set of constraint, or *static condensation*, modes, and $\boldsymbol{\Phi}$ is a set of fixed-boundary mode shapes. Truncating the modal coordinates at a cutoff frequency—thereby discarding the lowest-amplitude modes, which lie above the cutoff—gives

$$\begin{bmatrix} \mathbf{u}_b \\ \mathbf{u}_i \end{bmatrix} \simeq \boldsymbol{H} \begin{bmatrix} \mathbf{u}_b \\ \boldsymbol{\eta}^* \end{bmatrix}, \tag{26}$$

where $\boldsymbol{\eta}^*$ is the set of truncated, or *reduced*, modal degrees of freedom. Rewriting the equation of motion in terms of the reduced degrees of freedom gives the final working expression

$$\begin{bmatrix} \hat{\boldsymbol{M}}_{bb} & \hat{\boldsymbol{M}}_{bm} \\ \hat{\boldsymbol{M}}_{mb} & \hat{\boldsymbol{M}}_{mm} \end{bmatrix} \begin{bmatrix} \ddot{\mathbf{u}}_b \\ \ddot{\boldsymbol{\eta}}^* \end{bmatrix} + \begin{bmatrix} \hat{\boldsymbol{K}}_{bb} & \hat{\boldsymbol{K}}_{bm} \\ \hat{\boldsymbol{K}}_{mb} & \hat{\boldsymbol{K}}_{mm} \end{bmatrix} \begin{bmatrix} \mathbf{u}_b \\ \boldsymbol{\eta}^* \end{bmatrix} = \begin{bmatrix} \mathbf{f}_b \\ \mathbf{o} \end{bmatrix}, \tag{27}$$

where the $\hat{\boldsymbol{M}}_{**}$ terms comprise the reduced mass matrix $\hat{\boldsymbol{M}}$ and the $\hat{\boldsymbol{K}}_{**}$ terms comprise the reduced stiffness matrix $\hat{\boldsymbol{K}}$:

$$\hat{\boldsymbol{M}} = \boldsymbol{H}^{\mathrm{T}} \boldsymbol{M} \boldsymbol{H} \qquad \text{and} \qquad \hat{\boldsymbol{K}} = \boldsymbol{H}^{\mathrm{T}} \boldsymbol{K} \boldsymbol{H}. \tag{28}$$

Subscript m refers to the vibration modes of the body. External forces are assumed to act exclusively at the boundary nodes (that is, $\mathbf{f}_i = \mathrm{o}$). This result is the Craig-Bampton equation of motion and the reduced matrices in it are, with additional processing, the basis for the calculation of the state-space matrices. The reduced matrices are often provided by finite-element modeling software.

3.4.2 Rigid-Body Modes

The Craig-Bampton model captures not only the vibration modes of the flexible body but also the rigid-body modes—the translations and rotations of the body in the absence of deformation. Recall from section 3.1 that in the finite-element import method rigid-body motion is captured via the rigid-body model alone. You must therefore ensure that the deformation model, and the Craig-Bampton model upon which it is based, is free of rigid-body modes.

There are, in the general case, six rigid-body modes. A body in 3-D space can at a maximum translate in three perpendicular directions and rotate in three perpendicular planes. If the boundary nodes of the Craig-Bampton model have six degrees of freedom each, then the rigid-body modes can be removed by fixing one boundary node and setting all of its deflections to zero.

Consider again the Craig-Bampton equation of motion. Expanding the matrix terms to more explicitly show the degrees of freedom of the boundary nodes yields

$$\begin{bmatrix} \hat{M}_{11} & \cdots & \hat{M}_{1n} & \hat{M}_{1m} \\ \vdots & \ddots & \vdots & \vdots \\ \hat{M}_{n1} & \cdots & \hat{M}_{nn} & \hat{M}_{nm} \\ \hat{M}_{m1} & \cdots & \hat{M}_{mn} & \hat{M}_{mm} \end{bmatrix} \begin{bmatrix} \ddot{\mathbf{u}}_1 \\ \vdots \\ \ddot{\mathbf{u}}_n \\ \ddot{\boldsymbol{\eta}}^* \end{bmatrix} + \begin{bmatrix} \hat{K}_{11} & \cdots & \hat{K}_{1n} & \hat{K}_{1m} \\ \vdots & \ddots & \vdots & \vdots \\ \hat{K}_{n1} & \cdots & \hat{K}_{nn} & \hat{K}_{nm} \\ \hat{K}_{m1} & \cdots & \hat{K}_{mn} & \hat{K}_{mm} \end{bmatrix} \begin{bmatrix} \mathbf{u}_1 \\ \vdots \\ \mathbf{u}_n \\ \boldsymbol{\eta}^* \end{bmatrix} = \begin{bmatrix} \mathbf{f}_1 \\ \vdots \\ \mathbf{f}_n \\ \mathbf{o} \end{bmatrix}, \tag{29}$$

where subscripts 1 through n refer to the boundary nodes and each node is assumed to have six degrees of freedom. Suppose that you elect to fix boundary node 1 and set all of its possible deflections, three translational and three rotational, to zero. The Craig-Bampton equation, minus the duplicate degrees of freedom, becomes

$$\begin{bmatrix} \hat{M}_{22} & \cdots & \hat{M}_{2n} & \hat{M}_{2m} \\ \vdots & \ddots & \vdots & \vdots \\ \hat{M}_{n2} & \cdots & \hat{M}_{nn} & \hat{M}_{nm} \\ \hat{M}_{m2} & \cdots & \hat{M}_{mn} & \hat{M}_{mm} \end{bmatrix} \begin{bmatrix} \ddot{\mathbf{u}}_2 \\ \vdots \\ \ddot{\mathbf{u}}_n \\ \ddot{\boldsymbol{\eta}}^* \end{bmatrix} + \begin{bmatrix} \hat{K}_{22} & \cdots & \hat{K}_{2n} & \hat{K}_{2m} \\ \vdots & \ddots & \vdots & \vdots \\ \hat{K}_{n2} & \cdots & \hat{K}_{nn} & \hat{K}_{nm} \\ \hat{K}_{m2} & \cdots & \hat{K}_{mn} & \hat{K}_{mm} \end{bmatrix} \begin{bmatrix} \mathbf{u}_2 \\ \vdots \\ \mathbf{u}_n \\ \boldsymbol{\eta}^* \end{bmatrix} = \begin{bmatrix} \mathbf{f}_2 \\ \vdots \\ \mathbf{f}_n \\ \mathbf{o} \end{bmatrix}. \tag{30}$$

The first row and column of each matrix has been removed. Had boundary node 2 been fixed instead, the second row and column would have been removed. Note that if your choice of fixed boundary node changes, your choice of reference interface frame must too. See section 3.1.4 for more on the reference frame.

The state-space system comprising the deformation model is calculated in part from the matrices of equation (30). The calculations are discussed in greater detail in section 3.4.4.

3.4.3 Modal Damping

A true flexible body does not, in the absence of a driving force, vibrate forever. It loses energy with each cycle due to damping. The mechanisms of damping are varied and often difficult to characterize, but you can approximate their effects using a simple linear model. Adding to the reduced equation of motion a linear damping term $\hat{L}$ yields the expression:

$$\begin{bmatrix} \hat{M}_{bb} & \hat{M}_{bm} \\ \hat{M}_{mb} & \hat{M}_{mm} \end{bmatrix} \begin{bmatrix} \ddot{\mathbf{u}}_b \\ \ddot{\boldsymbol{\eta}}^* \end{bmatrix} + \begin{bmatrix} \hat{L}_{bb} & \hat{L}_{bm} \\ \hat{L}_{mb} & \hat{L}_{mm} \end{bmatrix} \begin{bmatrix} \dot{\mathbf{u}}_b \\ \dot{\boldsymbol{\eta}}^* \end{bmatrix} + \begin{bmatrix} \hat{K}_{bb} & \hat{K}_{bm} \\ \hat{K}_{mb} & \hat{K}_{mm} \end{bmatrix} \begin{bmatrix} \mathbf{u}_b \\ \boldsymbol{\eta}^* \end{bmatrix} = \begin{bmatrix} \mathbf{f}_b \\ \mathbf{o} \end{bmatrix}, \tag{31}$$

where $\hat{L}_{**}$ are submatrices of $\hat{L}$. Some modeling applications may provide the reduced damping matrix for a reduced finite-element model. Alternatively, you can obtain the damping matrix by direct calculation, using as a basis an appropriate model of damping. For a discussion of common damping models and of the matrix calculations that they entail, see *Fundamentals of Structural Dynamics*, by R. Craig and A. Kurdila[4].

A damping model in widespread use is that known as *modal damping*. This model assumes that the damping matrix can be diagonalized by a modal transformation. The values of the diagonal matrix elements are each calculated from a modal damping factor (ζ_i). The overall calculation can be summarized as follows:

1. Perform a modal analysis of the reduced finite-element model and obtain its normal mode shapes ($\boldsymbol{\Psi}$) and natural frequencies.
2. Transform the Craig-Bampton equation of motion—equation (31)—into modal coordinate space and add a modal damping term $\bar{\boldsymbol{L}}\dot{\mathbf{q}}$:

$$\bar{\boldsymbol{M}}\ddot{\mathbf{q}} + \bar{\boldsymbol{L}}\dot{\mathbf{q}} + \bar{\boldsymbol{K}}\mathbf{q} = \bar{\mathbf{f}}, \tag{32}$$

   where $\mathbf{q}$ are the modal degrees of freedom. The term $\bar{\mathbf{f}} = \boldsymbol{\Psi}^{\mathrm{T}}\hat{\mathbf{f}}$ is the modal force vector and the terms $\bar{\boldsymbol{M}}$, $\bar{\boldsymbol{L}}$, and $\bar{\boldsymbol{K}}$ are the modal mass, damping, and stiffness matrices. These matrices are related to their Craig-Bampton counterparts ($\hat{\boldsymbol{M}}$, $\hat{\boldsymbol{L}}$, and $\hat{\boldsymbol{K}}$) by the expressions

$$\bar{\boldsymbol{M}} = \boldsymbol{\Psi}^{\mathrm{T}}\hat{\boldsymbol{M}}\boldsymbol{\Psi}, \qquad \bar{\boldsymbol{L}} = \boldsymbol{\Psi}^{\mathrm{T}}\hat{\boldsymbol{L}}\boldsymbol{\Psi}, \qquad \bar{\boldsymbol{K}} = \boldsymbol{\Psi}^{\mathrm{T}}\hat{\boldsymbol{K}}\boldsymbol{\Psi}. \tag{33}$$

3. Construct the modal damping matrix. As mentioned previously, and akin to the mass and stiffness matrices, the damping matrix is assumed to be diagonalized by a modal transformation. Calculate the diagonal matrix elements by assuming them each to be a viscous damping term of the form $2\omega_i\zeta_i M_i$:

$$\bar{\boldsymbol{L}} = \begin{bmatrix} 2\omega_1\zeta_1 M_1 & & \\ & \ddots & \\ & & 2\omega_N\zeta_N M_N \end{bmatrix}, \tag{34}$$

where ω_i are the natural frequencies, ζ_i the modal damping factors, and M_i the elements of the (diagonal) modal mass matrix.

4. Transform the modal damping matrix into the reduced coordinate space employed in the Craig-Bampton equation. The final result is an expression of the form [4]

$$\hat{\boldsymbol{L}} = \left(\hat{\boldsymbol{M}}\boldsymbol{\Psi}\bar{\boldsymbol{M}}^{-1}\right)\bar{\boldsymbol{L}}\left(\bar{\boldsymbol{M}}^{-1}\boldsymbol{\Psi}^{\mathrm{T}}\hat{\boldsymbol{M}}\right), \tag{35}$$

where $\boldsymbol{\Psi}$ is the modal matrix of the flexible body.

3.4.4 State-Space System

Consider again the state-space representation of the deformation model (equations (18) and (19) of section 3.1.1):

$$\dot{\mathbf{x}} = \boldsymbol{A}\mathbf{x} + \boldsymbol{B}\mathbf{u} \qquad \text{and} \qquad \mathbf{y} = \boldsymbol{C}\mathbf{x} + \boldsymbol{D}\mathbf{u}.$$

In the finite-element import method, the states ($\mathbf{x}$) of this system are defined as the amplitudes, or participation factors, of the various vibration modes ($\boldsymbol{\eta}$):

$$\mathbf{x} = \begin{bmatrix} \boldsymbol{\eta}^* \\ \dot{\boldsymbol{\eta}}^* \end{bmatrix}. \tag{36}$$

Similarly, the inputs ($\mathbf{u}$) are defined as the deflections of the boundary nodes ($\mathbf{u}_b$)—or, equivalently, of the interface frames, relative to the common reference frame described in section 3.1.4:

$$\mathbf{u} = \begin{bmatrix} \mathbf{u}_\mathrm{b} \\ \dot{\mathbf{u}}_\mathrm{b} \\ \ddot{\mathbf{u}}_\mathrm{b} \end{bmatrix}. \tag{37}$$

Finally, the outputs ($\mathbf{y}$) are the internal forces and torques ($-\mathbf{f_b}$) that arise naturally in the body as a consequence of the nodal deflections. These forces and torques are opposite to the external applied loads that would produce those deflections:

$$\mathbf{y} = -\mathbf{f}_\mathrm{b}. \tag{38}$$

Casting the state-space matrices in terms of the reduced mass, damping, and stiffness matrices obtained from the reduced finite-element model gives, for the state matrix,

$$\boldsymbol{A} = \begin{bmatrix} O & I \\ -\hat{M}_{mm}^{-1}\hat{K}_{mm} & -\hat{M}_{mm}^{-1}\hat{L}_{mm} \end{bmatrix}; \tag{39}$$

for the input matrix,

$$\boldsymbol{B} = \begin{bmatrix} O & O & O \\ -\hat{M}_{mm}^{-1}\hat{K}_{mb} & -\hat{M}_{mm}^{-1}\hat{L}_{mb} & -\hat{M}_{mm}^{-1}\hat{M}_{mb} \end{bmatrix}; \tag{40}$$

for the output matrix,

$$\boldsymbol{C} = \begin{bmatrix} -\left(\hat{K}_{bm} - \hat{M}_{bm}\hat{M}_{mm}^{-1}\hat{K}_{mm}\right) & -\left(\hat{L}_{bm} - \hat{M}_{bm}\hat{M}_{mm}^{-1}\hat{L}_{mm}\right) \end{bmatrix}; \tag{41}$$

and for the direct-feedthrough matrix,

$$\boldsymbol{D} = \begin{bmatrix} -\left(\hat{K}_{bb} - \hat{M}_{bm}\hat{M}_{mm}^{-1}\hat{K}_{mb}\right) & -\left(\hat{L}_{bb} - \hat{M}_{bm}\hat{M}_{mm}^{-1}\hat{L}_{mb}\right) & -\left(\hat{M}_{bb} - \hat{M}_{bm}\hat{M}_{mm}^{-1}\hat{M}_{mb}\right) \end{bmatrix}. \tag{42}$$

3.5 Examples

3.5.1 Flexible Cantilever Beam

Consider the flexible cantilever beam first discussed in section 2.4.1. The properties of the beam are those described there. The loading conditions are likewise the same—one a distributed gravitational load (associated with a gravitational acceleration 100 times that of Earth), the other a beam subjected to an upward point force of `20 N` in a zero-gravity environment.

Model Parameters The beam model considered here contains three interface frames. The inertia of the beam is split over the interface frames in sizeable chunks—the conceptual case described in item c of section 3.3.2. As is encouraged in section 3.1.4, the reference frame of the body is located at the center of the beam.

The deformation model is based on a finite-element model reduced by the Craig-Bampton method to the first 20 vibration modes. The feedback loops between the deformation model and the deflection joints each contain a first-order filter of time constant `1e-7 s`. The filter is based on the transfer function described in section 3.3.1.

Modal damping is included in the model in the matrix form described in equation (34). The damping parameter ζ used to construct the damping matrix is set to a value of `0.05`.

Simulated Deflections Figure 20 shows the time-varying deflections of the free end of the beam under a uniform gravitational load (case **I**) and a tip point load (case **II**). The beam is lightly damped and reaches equilibrium in each case after approximately five seconds. The point force is removed after five seconds of simulation, allowing the beam to return to its natural state of zero deflection. The return to equilibrium is governed by the internal forces of the beam alone (gravity is ignored).

The simulation results show that the free end of the beam settles at an equilibrium deflection of `-0.0183 m` under a uniform gravitational load and `0.0164 m` under an upward-facing point load. Compare these values to the analytical predictions of `-0.0191 m` for a uniform gravitational load and `0.0165 m` for an upward-facing point load, respectively (see section 2.4.1).

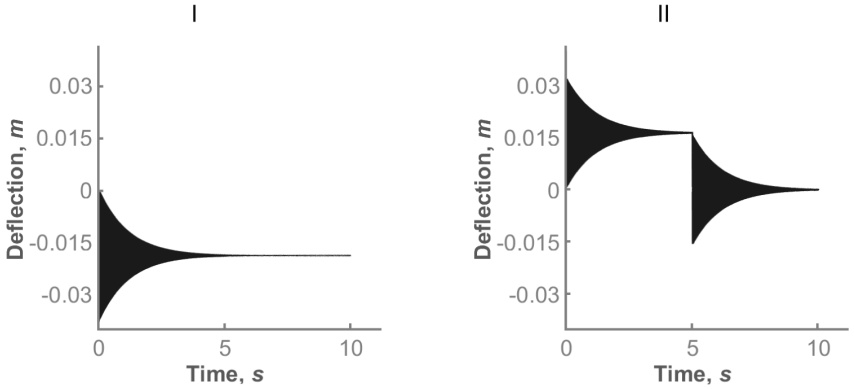

Figure 20: Tip deflection due to a distributed gravitational load (left) and to an upward point load (right)

3.5.2 Crank-Slider with Flexible Links

Consider the crank-slider mechanism first discussed in section 2.4.2. The characteristics of the mechanism are those described there, with the crank and coupler links both modeled as flexible bodies. The mechanism is driven by the applied torque of A. Shabana. Two cases are considered—one with collision against a hard stop and one without.

Model Parameters The crank and coupler are modeled by the finite-element import method and given three interface frames each. The remaining bodies are treated as rigid. The inertias of the flexible bodies are split over the interface frames in sizeable chunks (item c of section 3.3.2). For improved accuracy, the reference frames are each placed at a central location on the body.

The deformation model is based on a finite-element model reduced by the Craig-Bampton method to the lowest-frequency vibration modes. The feedback loops between the deformation model and the deflection joints each contain a first-order filter of time constant `1e-7 s`. The filter is based on the transfer function described in section 3.3.1.

Modal damping is included in the model in the matrix form described in equation (34). The damping parameter ζ used to construct the damping matrix is set to a value of `0.05`.

Simscape Multibody Model Figure 21 shows a Simscape Multibody model of the crank-slider mechanism. The crank, coupler, and slider, connect to each other and to the world by means of joints. The driving torque is applied directly to the revolute joint that connects the crank to the world. The hard-stop force is applied directly to the prismatic joint that connects the slider to the world.

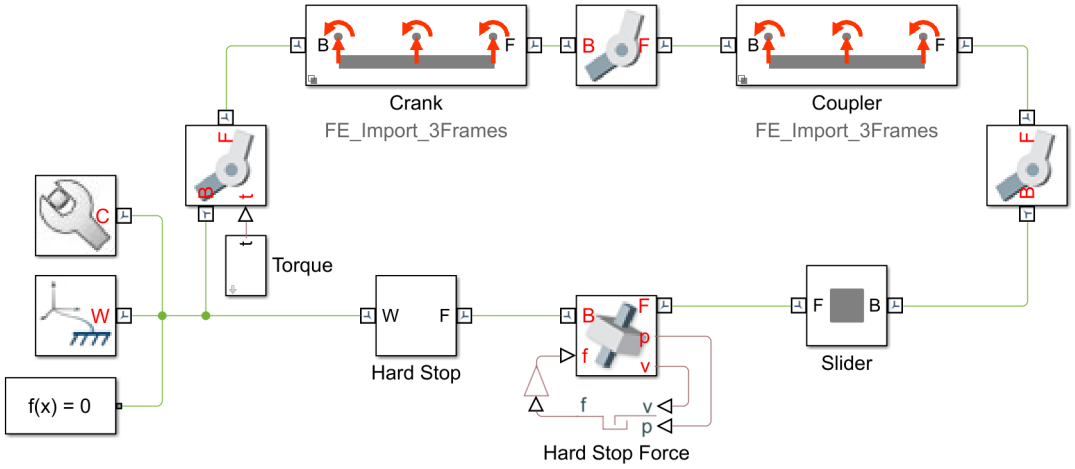

Figure 21: Simscape Multibody model of a crank-slider mechanism

Figure 22 shows the Simscape Multibody representation of one flexible body—the coupler. A Solid block (named **Rigid Body**) comprises the rigid-body model. A Simulink State Space block (**State Space System**) comprises the deformation model. The two models connect through deflection joints, each enclosed in a Simulink Subsystem block (**Deflection Joint 1–2**). A third Simulink Subsystem (**Rigid Connection**) denotes the connection to the chosen reference frame.

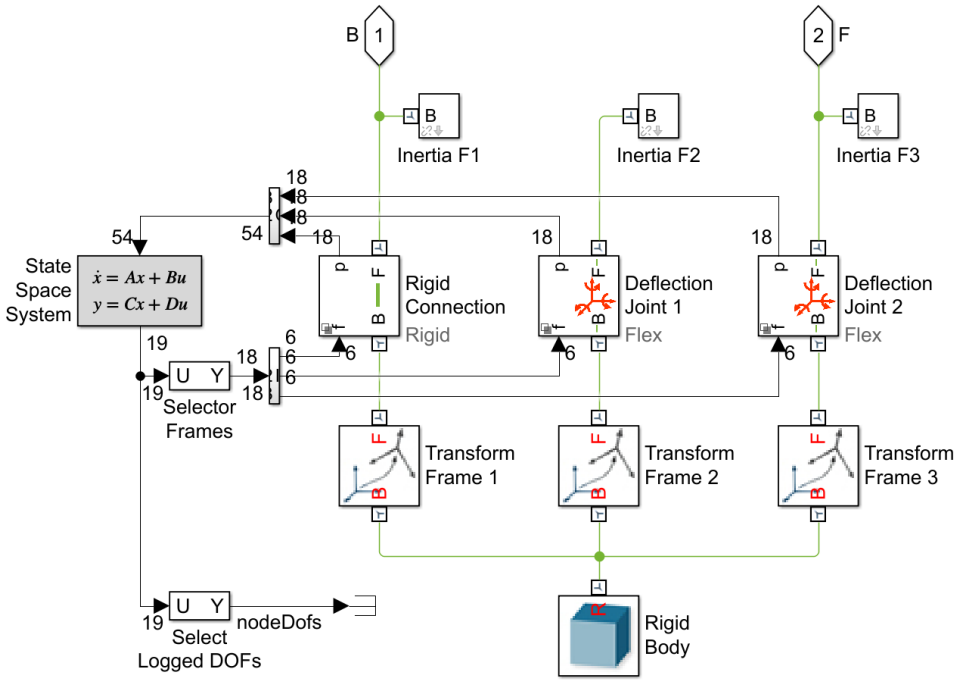

Figure 22: Simscape Multibody model of a flexible coupler

The interface frames are denoted by Simscape Physical Connection blocks (named **B**, **M**, and **F**). The interface inertias are specified through Simulink Subsystem blocks (**Inertia F1**–**F3**), each enclosing a Solid block. The three Rigid Transform blocks (**Transform Frame 1**–**3**) merely define the placement of the frames through which the rigid-body model connects to the deflection joints.

Simulated Deflections Figure 23 overlays the simulation results obtained here using the finite-element import method (curve **B**) on those published by A. Shabana (curve **A**). The curves each correspond to the transverse deflection measured at the midpoint of the coupler link with respect to an imaginary line drawn between the longitudinal ends of the same link.

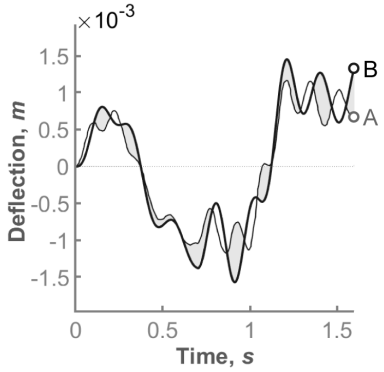

Figure 23: Comparison to Shabana[2] simulation results (**A**: Shabana, **B**: Simscape Multibody)

Figure 24 shows the simulation results obtained from a model with an obstacle—a translational hard

stop—placed in the path of the slider. Contact occurs shortly after the 0.5-second mark, inducing in the coupler link the vibrations shown. As before, the results correspond to the transverse deflection measured at the midpoint of the coupler link. The oscillations decay at a rate determined by the damping matrix used in the model.

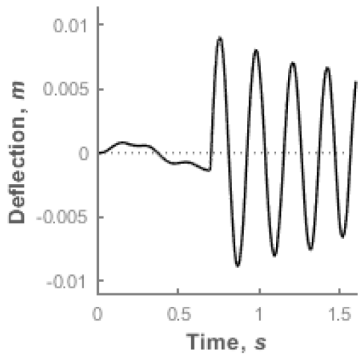

Figure 24: Coupler deflection due to contact

Simulation Accuracy The simulation results depend closely on the configuration of the model. The number of interface frames, the number of vibration modes, the location of the reference frame (that to which the rigid-body model is fixed), and the partitioning of inertia among the interface frames can all impact the dynamics of the flexible body.

Figure 25 shows, in a model without an obstacle, the effect of changing the number of interface frames. Curve **A** corresponds to a model with three interface frames per flexible body. Curve **B** corresponds to a model with five interface frames per flexible body. Increasing the number of interface frames improves the accuracy of the model. Results by A. Shabana are overlaid in bold. The crank and coupler are each modeled with a centrally located reference frame and equitably partitioned interface inertias.

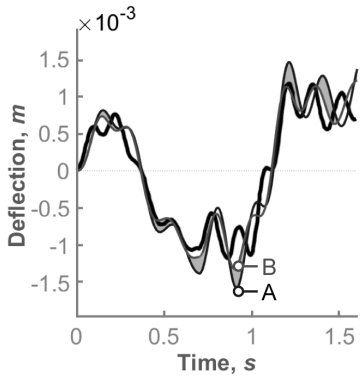

Figure 25: Effect of changing the number of interface frames (**A**: three interface frames, **B**: five interface frames)

Figure 26 shows the effect of partitioning the inertia over the various interface frames. Curve **A** corresponds to a model in which the interface inertias are negligible. Curve **B** corresponds to a model in which inertia has been more equitably distributed over the interface frames. Partitioning the inertia equitably over the

interface frames improves the accuracy of the model. Results by A. Shabana are overlaid in bold. The crank and coupler are each modeled with three interface frames and a centrally located reference frame.

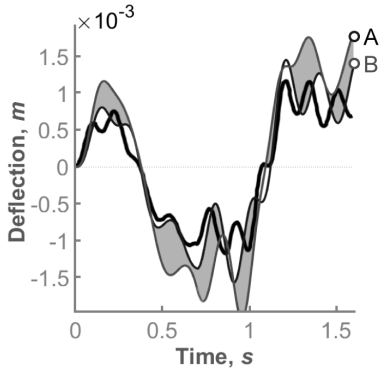

Figure 26: Effect of partitioning the inertia over the interface frames (**A**: negligible interface inertias, **B**: sizeable interface inertias)

The selection of reference frame can have an especially significant impact on your simulation results. Figure 27 shows the effect of switching the reference frames of the flexible bodies each from an interface frame at an end (curve **A**) to one near the center (curve **B**). Placing the reference frame at a central location improves the accuracy of the model. Results by A. Shabana are overlaid in bold. The crank and coupler are each modeled with three interface frames and equitably partitioned interface inertias.

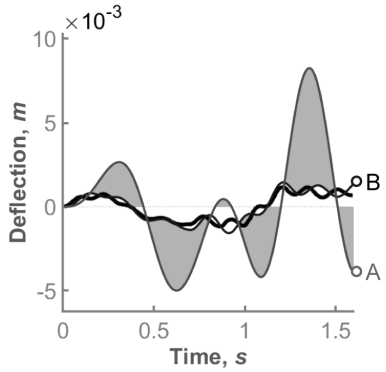

Figure 27: Effect of changing the placement of the reference frame (**A**: reference frame near tip, **B**: reference frame near center)

Visualization Results Figure 28 shows the visualization results obtained from a Simscape Multibody model of the crank-slider mechanism. The coupler is modeled as a rigid body in case I, as a flexible body with three interface frames in case II, and as a flexible body with five interface frames in case III. Inertia is split over the interface frames in cases II and III. In each case, the model is shown as it appears an instant (`0.05 s`) after collision with the hard stop.

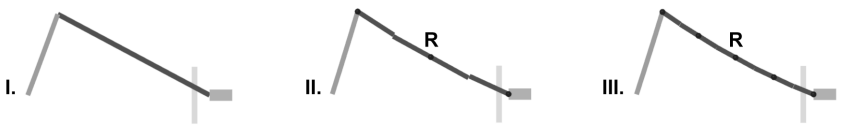

Figure 28: Visualization with the coupler as a rigid body (I) and as a flexible body with three (II) and five (III) interface frames

Deformation is made evident in this figure in two ways. First, the interface inertias are modeled as solids with geometry, each a section of the coupler beam. These geometries comprise the entirety of the coupler in the visualization results. Second, spherical markers are appended to the interface frames, making the deflections of those frames more evident.

The coupler is naturally undeformed in case I. It is slightly deformed in case II but, due to the small number of interface frame solids, its visualization has a staggered appearance. The same deformation is evident in case III, now with smoother visualization results produced by the greater number of interface frame solids used.

4 Conclusion

You can represent a flexible body in a multibody model using lumped-parameter and finite-element import methods. The lumped-parameter method discretizes the body into flexible units, each comprising two mass elements coupled through a joint with an internal spring and an internal damper. This method provides a simple solution for bodies with slender geometries, with an accuracy that depends largely on the number of flexible units used.

The finite-element import method splits the flexible body into a rigid-body model and a deformation model and superposes their respective motions. The deformation model is implemented as a state-space system created from data that you obtain from a reduced finite-element model. This method provides a superior solution for general 3-D geometries, with an accuracy that depends on the number of interface frames, the partitioning of mass properties, the location of the reference frame, and the number of vibration modes.

The examples show that the lumped-parameter method improves in accuracy when the number of flexible units increases in number—though above a certain discretization level any subsequent increases in accuracy become negligible. Similarly, the finite-element import method improves in accuracy when the interface frames increase in number, when the inertia of the body is more equitably split over the interface frames, and when the reference frame is centrally located on the body.

References

[1] *Simscape Multibody Documentation* . MathWorks. http://www.mathworks.com/help/physmod/sm/index.html

[2] Shabana, Ahmed A. *Dynamics of Multibody Systems* . 4th ed. Cambridge University Press, 2013.

[3] Craig, Roy R. and Bampton, Mervyn C. *Coupling of Substructures for Dynamic Analyses* . AIAA Journal 6, no. 7 (1968): 1313–1319.

[4] Craig, Roy R. and Kurdila, Andrew J. *Fundamentals of Structural Dynamics* . 2nd ed. John Wiley & Sons, 2006.

[5] Miller, S. *Flexible Body Models in Simscape Multibody* . MathWorks. https://www.mathworks.com/matlabcentral/fileexchange/47051